

Anechoic Dome Chamber

A Supporting Structure to Antenna Dome 2.0

John de Graaf
Rui Mao

Delft University of Technology



Anechoic Dome Chamber

A Supporting Structure to Antenna Dome 2.0

by

John de Graaf
Rui Mao

to obtain the degree of Bachelor of Science
at the Delft University of Technology.

| | | |
|-----------------------|--------------------------|--------------------------------------|
| Student name, number: | John de Graaf | 4351525 |
| | Rui Mao | 5041635 |
| Project duration: | April, 2022 – June, 2022 | |
| Thesis committee: | Dr. Marco Spirito, | TU Delft, supervisor |
| | Richard Coesoij MSc, | TU Delft, daily-supervisor |
| | Dr. Ryoichi Ishihara, | TU Delft, graduation committee chair |
| | Dr. Massimo Mastrangeli, | TU Delft, graduation committee |

Cover: Outside of the minidome

An electronic version of this thesis is available at <http://repository.tudelft.nl/>.

Abstract

In this thesis, the realization and qualification of an anechoic dome chamber for 5G antenna's is discussed. As with audio, where no echoes or noise from outside is wanted when listening to music, when characterizing an antenna it must be prevented to get internal reflections or electromagnetic (EM) radiation from outside.

For this reason, a measurement setup was simulated, using that setup, different absorbers were tested and characterized. And a Faraday cage shielding is designed and evaluated, to remove EM interference.

To make the anechoic chamber physically possible, rebuilding the minidome was also required, so that the absorber and Faraday cage could be mounted on the inner wand of the dome. Eventually, a suitable test environment for 5G antenna's is build.

In the end, the assessment of the absorbing materials was completed, and the chamber achieved all requirements. Despite the space of improvement, the idea of building an anechoic chamber is successfully verified.

Preface

As the final part in our Bachelor of Electrical Engineering, we were the last 8 weeks busy on our Bachelor Graduation Project. The chosen subject of an antenna dome was great to get hands-on work with cutting edge technology, it also helped to understand different aspects of mm-wave radiation and in 5G technology. While there were ups and downs during the project, it has given a lot of pride and satisfaction to complete the project in the short allocated time.

We would like to thank everyone who helped to support this project: for providing supervision, ideas and advice, coaching us, helping in the lab, making tools available or helping to make it possible to rebuild the dome. It all helped us to better understand and be able to act as an Engineer. And we look happy back on a great project that gives us the opportunity to obtain our bachelor degree.

*John de Graaf
Rui Mao
Delft, June 2022*

Contents

| | |
|----------------------------------------------|-----------|
| Abstract | i |
| Preface | ii |
| 1 Introduction | 1 |
| 1.1 General Information | 1 |
| 1.2 State-of-the-Art Analysis | 1 |
| 1.2.1 Absorbing Material Characterization | 1 |
| 1.2.2 Mathematical Definition of the Problem | 2 |
| 1.3 EMI Shielding | 3 |
| 1.4 Document Structure | 4 |
| 2 Program of Requirements | 5 |
| 2.1 Non-functional Requirements | 5 |
| 2.2 Functional Requirements | 5 |
| 3 Methods | 6 |
| 3.1 Characterization of Absorbing Materials | 6 |
| 3.1.1 Simulations | 7 |
| 3.1.2 Physical Setup | 9 |
| 3.1.3 Codes Design | 10 |
| 3.2 Faraday cage | 11 |
| 3.2.1 Physical Setup | 12 |
| 3.3 Anechoic Chamber | 13 |
| 3.3.1 Rebuilding the Mini-dome | 13 |
| 3.3.2 Assessment of the Anechoic Chamber | 14 |
| 4 Results | 15 |
| 4.1 Absorbing Material Assessment | 15 |
| 4.1.1 Verification of MatLab Codes | 15 |
| 4.1.2 Time Gating | 16 |
| 4.1.3 Absorbing Material Comparison | 18 |
| 4.2 Assessment of the Chamber | 19 |
| 4.2.1 Faraday shielding Measurement | 19 |
| 4.2.2 S11 Measurement | 20 |
| 5 Conclusion and Discussion | 21 |
| 5.1 Conclusion | 21 |
| 5.2 Discussion | 21 |
| 5.3 Recommendations | 22 |
| A Source Code | 26 |
| A.1 Functions | 26 |
| A.1.1 AssembleComplex | 26 |
| A.1.2 Analysis | 27 |
| A.2 Scripts | 28 |
| A.2.1 DataAssemble | 28 |
| A.2.2 RunAnalysis | 29 |
| B Additional Data | 31 |
| B.1 Addition Data of Simulations | 31 |
| B.2 Addition Data of Absorbing Materials | 32 |

Introduction

1.1. General Information

The size of 5G infrastructure has been growing rapidly since 2020 [1], which also brings challenges of characterization of millimetre wave (mm-wave) antennas [2]. So far, many characterization methods of mm-wave antennas use a single measurement antenna as receiver, which is stationary or driven by robotic arms [2][3]. One of the drawbacks of single antenna receiver is the difficulty to perform simultaneous measurements in multiple directions. On the other hand, many experiment setups consist of multiple in-phase antennas [4]. Among all other multiple antenna setups, the antenna dome model has the potential to perform 3D real time characterization [5].

The current design of the last mentioned dome consists of an aluminium structure and a phased antennas array. For the time being, such a setup suffers from external EM-disruption. To improve its electromagnetic coherence, a method is designed that converts the current design into an anechoic chamber, which is further referred as 'the chamber' in the rest of this thesis. An anechoic chamber is a critical equipment that can significantly increase the accuracy of the measurement by shielding away the external influence and reduce the internal reflection [6]. Furthermore, as the most critical component of the chamber, the absorbing material should be carefully chosen and examined.

1.2. State-of-the-Art Analysis

1.2.1. Absorbing Material Characterization

Research has been done to the absorbing material characterization techniques. The main challenge is to separate the signal affected by the absorber under test, and compare it with the reference. To achieve this goal, time-gating technique can effectively separate contribution of the signal affected by absorbing material and the reference signal [7][8][9].

Time-gating techniques are based on Fourier Transform and inverse Fourier Transform. They are capable of converting signals from frequency domain (Power Spectral Density) to time domain (Transient Response), or the other way around. Once the Time of Arrival (ToA) of those signals is known, which can usually be calculated via the speed of light and the length of the travel path, the signals can be easily located in a much smaller interval than the whole time interval of measurements. Its advantage is that the most relevant signal can be then extracted, and the irrelevant intervals are then filtered out. This not only helps to identify near field signal for detailed analysis [10], but also makes far field measurements less sensitive to arbitrary time domain noise.

Time-gating techniques also provide two options to the assessment. One option is to keep the path unchanged but carry out two measurements, with and without absorber separately [7]. The other option is to design different paths but scan both paths simultaneously. Both are applicable in characterization of absorbing materials. Different travel paths designs are shown in Figure 1.1.

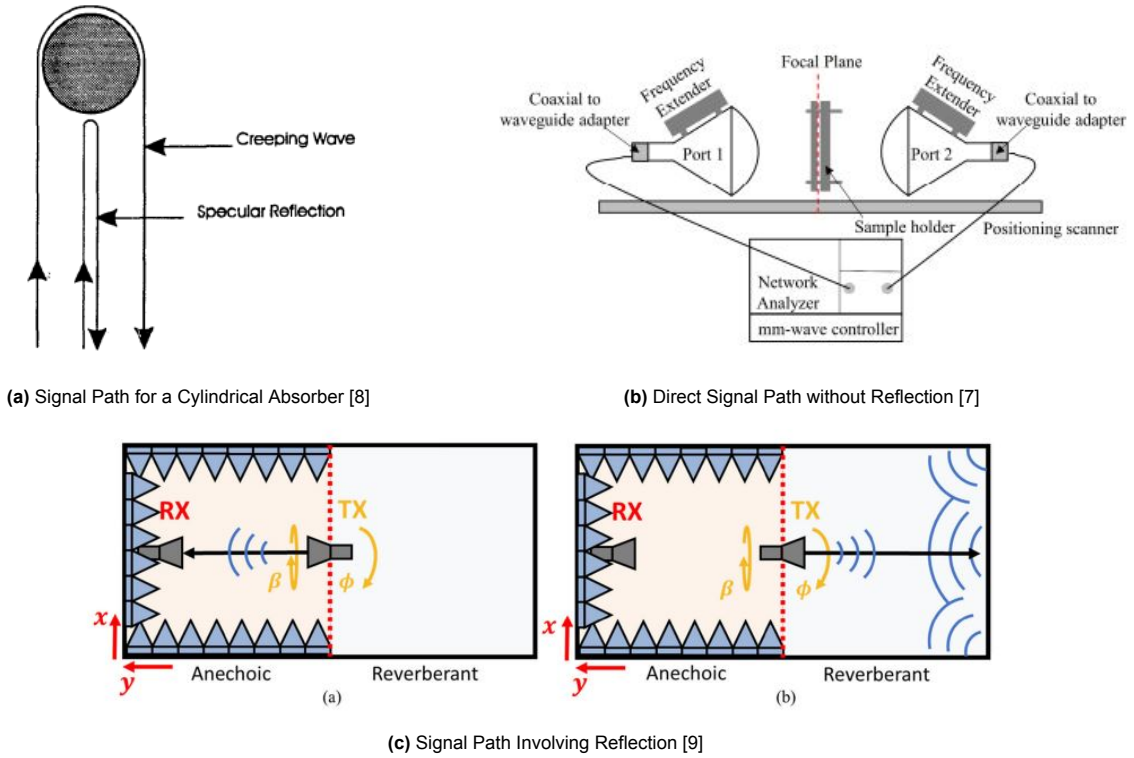


Figure 1.1: Different Signal Path Designs in Previous Works

1.2.2. Mathematical Definition of the Problem

The problem is defined as a characterization problem as shown in Figure 1.2b. With a physical setup according to Figure 1.2a, the signal sent out from the antenna is going to go through the absorbing plate and reflected by the metal plate, then received by the sender again.

Time-gating technique has general algorithm flow as shown in Figure 1.3. The physical setup is shown in Figure 1.2a. With a certain method, the response of the absorbing material $A(f)$ is desired. As always, the total response also include a noise created by many factors.

The starting point is the measured response power spectral density (PSD) $Y(f)$. $Y(f)$ contains a combination of all responses throughout the time duration in the environment. The first step of approaching the data is to transform it into the time domain using inverse Discrete Time Fourier Transform [11].

$$y(t) = y(nT) = \int_{-\frac{1}{2}}^{\frac{1}{2}} Y(f) e^{i2\pi f t} df, T = \frac{1}{f_{end}} \quad (1.1)$$

Here $g(t)$ is the time response, $y(nT)$ is the discrete time response, T is the step size of the time response and f_{end} is the highest sample frequency. Because the knowledge about travel path length l , an observable peak at the time of arrival (ToA) t_a is expected. Then the signal $y(t)$ can be rewritten as:

$$y(t) = p(t) + n_t(t) \quad (1.2)$$

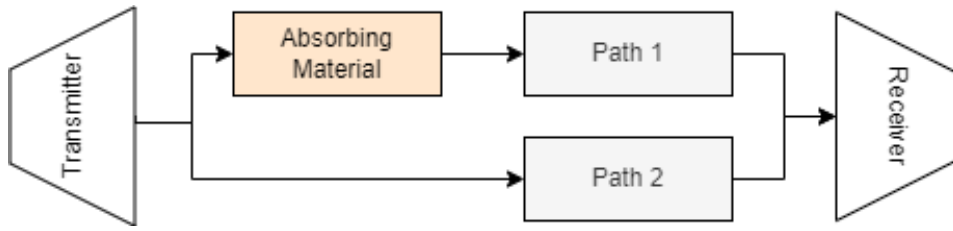
Here $p(t)$ is the expected clean signal peak received and $n_t(t)$ is the noise signal. Further, the expected ToA can be calculated using formula

$$t_a = \frac{l}{c} = \frac{2d}{c} \quad (1.3)$$

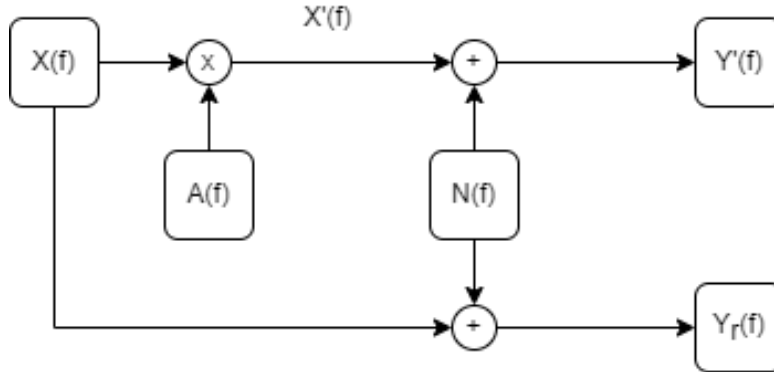
Here c the propagation speed of light in the vacuum, d is the height of the antenna to the metal plate and l is the propagation length.

A small interval centered at t_a , which should contain a clear peak and as little other material as possible, is the target of analysis. By windowing it the uninteresting time domain signals can be suppressed.

$$y'(t) = W(t)y(t) \quad (1.4)$$



(a) Illustration of the physical setup



(b) The signal flow chart. $X(f)$ and $Y(f)$ are the PSD of the transmitter and receiver side. $A(f)$ is the attenuation of the absorbing material and $N(f)$ is the summation of all the rest of the effects. $f \in [f_{start}, f_{end}]$.

Figure 1.2: The problem definition.

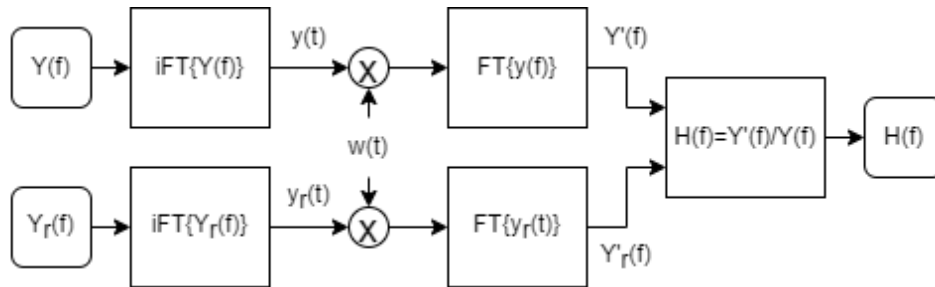


Figure 1.3: Data Processing

Here $y'(t)$ is the result of windowing, $W(t)$ is the window function. The resulting signal $y'(t)$ can then be transformed back to the frequency domain using Discrete Time Fourier Transform (DTFT).

$$Y'(f) = \sum_{-\frac{1}{2}}^{\frac{1}{2}} y'(t)e^{-i2\pi t} \tag{1.5}$$

At this step, the response only consists of the PSD of the signal affected by the material. In order to obtain the pure spectrum, which means without other environmental influence, a spectrum $Y_r(f)$ with only metal plate is going to be used. After the same process to obtain $Y'(f)$, the resulting signal $Y'_r(f)$ contains only the environmental influence. The pure response $H(f)$ can be obtained from:

$$H(f) = \frac{Y'(f)}{Y'_r(f)} \tag{1.6}$$

1.3. EMI Shielding

For antenna's characterization, a clean EM environment is necessary. As only then the Radiated emissions can be assured to come from the Antenna under test (AUT) [12]. Beside using absorbing material to remove unwanted reflections inside the anechoic chamber, this chamber must be shielded from external EM radiation. A way to do this is by using a Faraday cage.

A couple of rules for making such a Faraday cage are that the openings are below $1/20th$ of the wavelength, or for even higher quality below $1/50th$ [13]. Given the frequency from 28 GHz where the 5G antenna's are based upon, the wavelength [m] is calculated with formula below, where c is the speed of light [$3 \times 10^8 m/s$].

$$\lambda = \frac{c}{f} = 10.7mm \quad (1.7)$$

For 5G there is also research done to EMI shielding [14], and particular research is also done how ventilation holes can be incorporated [15]. This could be handy in case the dome is fitted with an antenna network that is used to measure the radiation from the AUT. As such a network could dissipate heat, possible needing ventilation to radiate it away. Which at the given possible cage openings of $0.2mm$ will be hard to achieve, since little airflow is possible.

To find out the required thickness of the metal used for the Faraday cage, the skin depth needs to be calculated using the formula below [16][17].

$$\delta = \sqrt{\frac{\rho}{\pi f \mu_0 \mu_r}} \quad (1.8)$$

Where δ is the skin depth [m], ρ the resistivity of the conductor [Ωm], f the frequency [Hz], μ_0 the permeability of free space [$4\pi \times 10^{-7} H/m$] and μ_r the relative magnetic permeability of the conductor [H/m]. After calculation, the skin depth of aluminium is determined to be $0.489\mu m$ and for copper $0.390\mu m$ at 28 GHz.

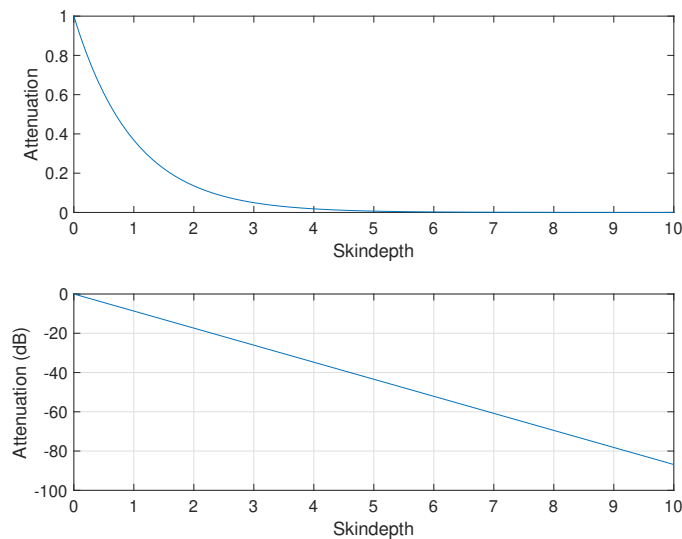


Figure 1.4: The attenuation, a multiple of the skin depth gives, linear and on a dB scale.

Using the skin effect, which depicted that in a good conductor, the electric field decays by $1/e$, or 36.8% after travelling a distance of one skin depth [17]. This can then be used to graph the attenuation that a multiple of the skin depth will give.

1.4. Document Structure

This thesis is further divided into several chapters. Chapter 2 defines all the requirements of this project. Chapter 3 explains the methods used in each step leading to the anechoic chamber. Chapter 4 shows the results of assessments. Finally, Chapter 5 presents the conclusion of the project, as well as a brief discussion and some recommendations.

2

Program of Requirements

This chapter aims to list all requirements for designing the chamber in the project. The following sections are going to explain the requirements in more details. Section 2.1 is going about non-functional requirements. Section 2.2 is about the functional requirements.

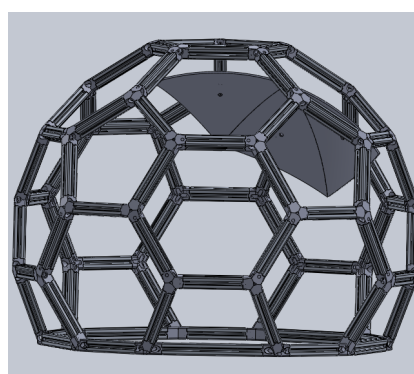
2.1. Non-functional Requirements

As mentioned in the introduction, one of the existing design has a dome structure. At the time being, the structure has been improved as shown in Figure 2.1a. In this project, the aim is to construct an anechoic chamber for the improved version to improve the signal quality. The requirements to the chamber are listed below:

1. The structure of the dome needs to be updated, to create an inner shell where the anechoic chamber will be build on, while still keeping a modular structure.
2. Before constructing the chamber, an analysis of all possible absorption and shielding materials should be provided.
3. If all functional requirements are met, the weight of the dome should be as low as possible.
4. (Optional) An analysis of the absorbing material under different reflection path lengths is desirable if the time allows.



(a) The current minidome



(b) Render of the redesigned minidome

Figure 2.1: Versions of the minidome design

2.2. Functional Requirements

The functional requirements are listed below

1. The chamber is based for use with 5G NR antenna's in the FR2 band, thus in a frequency range of 26.5 - 29.5 GHz.
2. The attenuation of the material on the chamber should be equal or lower than -5dB if the absorber is based upon a paint, or -10 dB when a stock absorber is used.
3. The shielding of the Faraday cage should be equal to or lower than -30 dB.

3

Methods

To achieve the requirements listed in the previous chapter, the project was split into 3 parts: the evaluation of the absorbing materials, the design of a Faraday cage and the construction of the chamber with chosen absorbing material and shielding possible. Hence, this chapter consists of three sections. First, section 3.1 explains the methods of comparing absorbing materials. After that, section 3.2 explains the assessment of the Faraday cage. Finally, section 3.3 explains the realization of the Anechoic Chamber and the measurements that are done on the assembled dome.

3.1. Characterization of Absorbing Materials

The aim of this part is to assess different types of absorbing materials, which are MMW-1 flexible foam, MMW-2 flexible foam both from Cuming Microwaves [18] and Gigahertz Solutions CFA40-5 paint [19] with optional carbon grains. This section is further divided into several subsections. Subsection 3.1.1 explains the choice of our setup based on ADS simulation. Subsection 3.1.2 shows details of the physical setup. Finally, Subsection 3.1.3 explains the MATLAB codes designed to finish the measurements.

There are 2 measurement setups are possible:

1. Measure one-port S_{11} response of one antenna which is at a given angle and distance from the absorber. A schematical setup of this is visible in figure 3.1a.
2. Measure two-port S_{12} response of two identical antennas where there is a certain angle between them, such that the second antenna broadside lays in the first null of the first antenna. And thus, since the antennas are identical, the first antenna broadside lays in the second antenna first null, resulting in a dual null attenuation. The absorber lays in the intersection point of the 2 broadside lines from the antenna's. A render of this setup is visible in figure 3.1b.

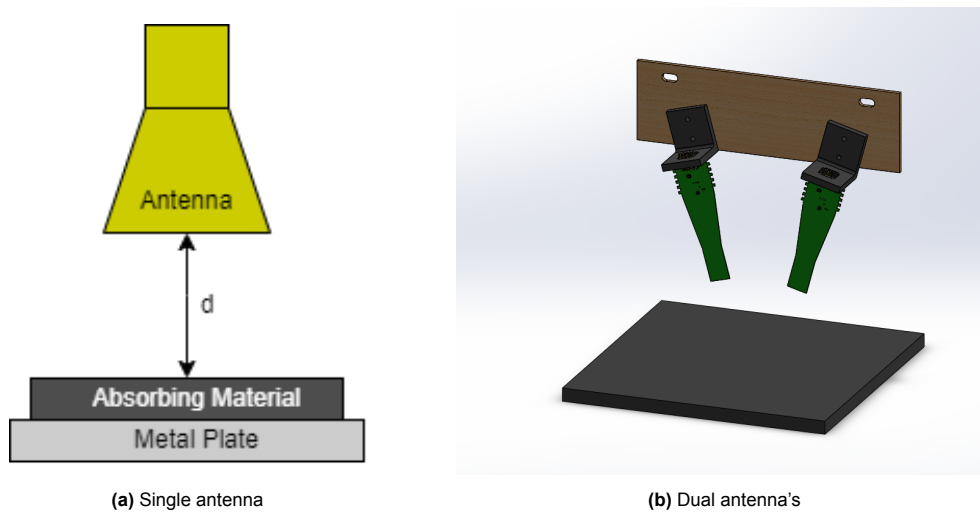


Figure 3.1: Possible antenna setups to test the absorber

3.1.1. Simulations

To test which setup was the best to use, simulations of both setups were made in ADS. The simulation parameters can be found in the appendix at figure B.1. But in short, the measurement setup was built twice in each simulation, ones with a -10 dB absorber+reflector under the antenna, and ones without that absorber. This should yield to a difference in received power of 20 dB, since the signal penetrates the absorber, gets reflected and travels back through the absorber. The results of these simulations are shown in figures 3.2, 3.3 and 3.4. On the left part of those figures, the S-parameters are shown without any further processing. On the right part of the figures, there is Time gating applied. It can be seen from figure 3.2 that time gating is necessary to see the effect of the -20dB absorption, as on the left side hardly any difference in power is received.

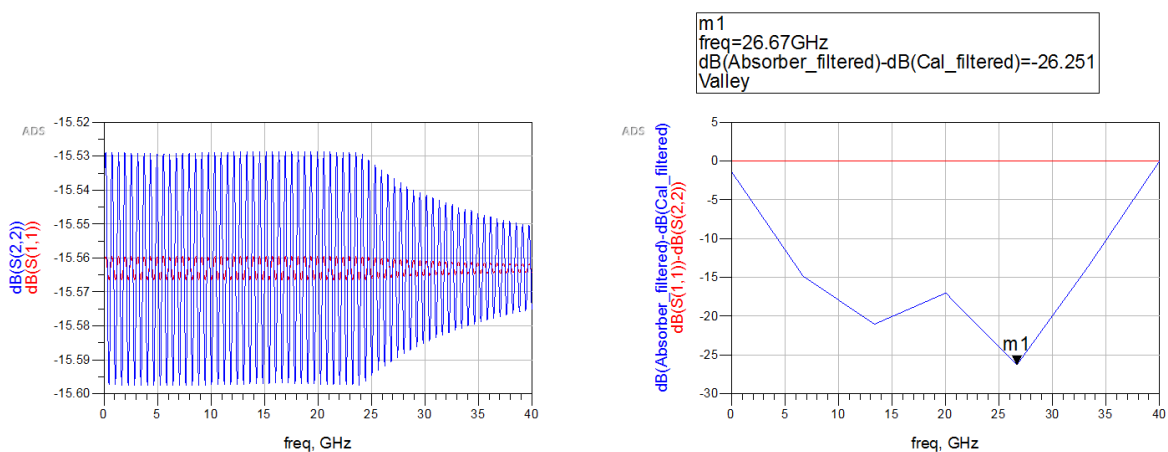


Figure 3.2: Simulation result of single antenna setup

When changing to the dual antenna setup, it depends on how much coupling is between the antenna's. In figure 3.3 a coupling loss factor of 50 dB. Here still time gating is needed to see the effect of the absorber. While in figure 3.4 with a coupling loss factor of 100 dB, this effect is even visible without time gating. However, using time gating does clean up the resulting signal.

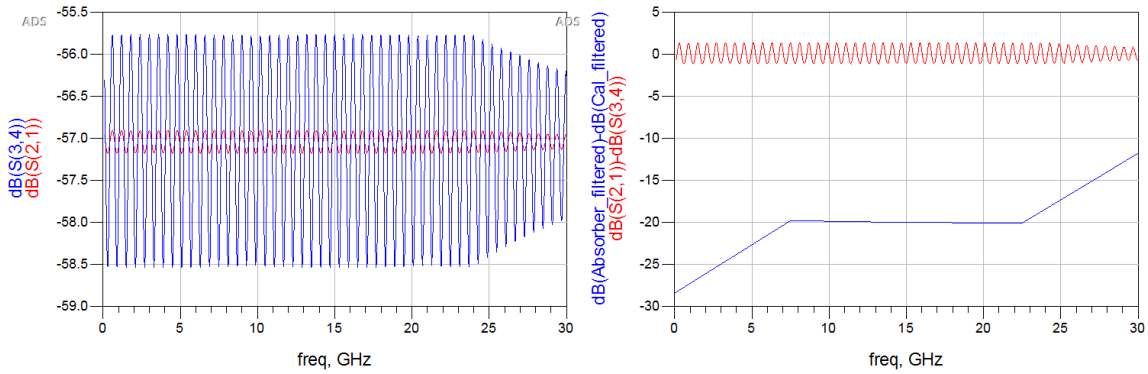


Figure 3.3: Simulation result of dual antenna setup with 50 dB coupling loss

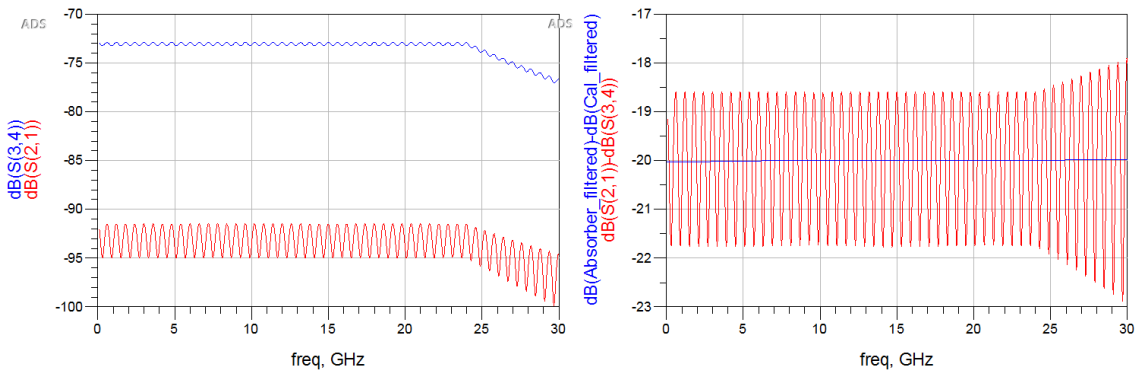


Figure 3.4: Simulation result of dual antenna setup with 100 dB coupling loss

Since the antenna's that are proposed for use in the dual antenna setup, Vivaldi antenna's with the radiation pattern shown in figure 3.5, that would give a coupling loss of 50 dBc when the antenna's are placed in the setup from figure 3.1b, where the antenna's are placed at an angle of 30 or 35 degree from each other's broadside. This coupling loss is calculated using figure 3.5 and see where the first null of the copolar waveform is situated and compare the gain at that angle with the broadside. These gains can then be added, to give the coupling loss.

This then would conclude that time gating is needed for either single or dual antenna setup. Since a single antenna is easier to place and to move to different heights, as no change of the holder is needed, the physical setup was chosen to be based upon the single antenna setup.

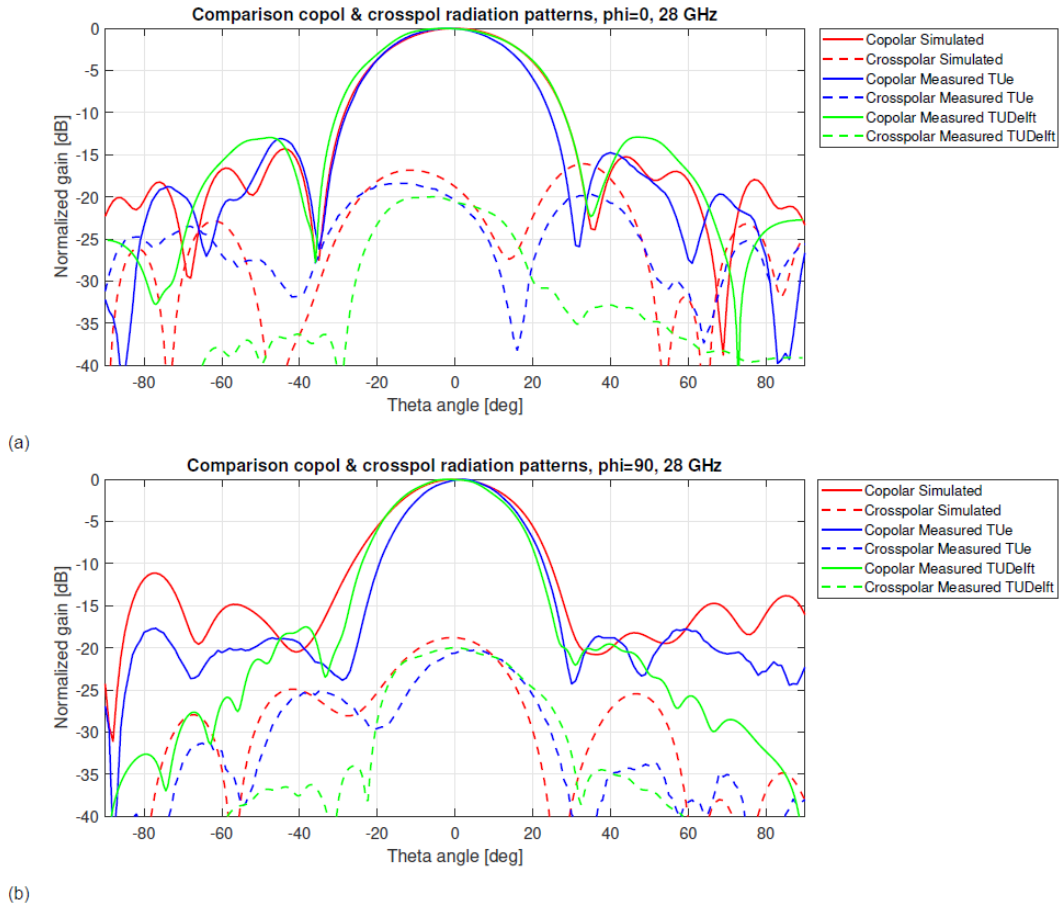


Figure 4.28: Measured radiation patterns using both measurement setups. Both the copolar and crosspolar patterns are shown.

Figure 3.5: Picture showing the radiation pattern from the Vivaldi antenna [5]

3.1.2. Physical Setup

Instruments

In this experiment, a Flaan 22240 Standard Gain Horn was used, as it covers the frequency range of 26.4GHz to 40.1GHz. To measure its response, the KEYSIGHT PNA Network Analyzer NS224B was used in this experiment. Besides, GORE® PHASEFLEX® Microwave/RF Test Assemblies are used to connect the PNA and the horn antenna, which were calibrated by Anritsu K Connector Calibration Kit 3652 Series.

Measurement Procedure

The measurement procedure is described in the list below. As the interested frequency was around 28 GHz, the measurement was calibrated from 23 to 33 GHz. In order to choose a proper height, the far field distance [m] needs to be calculated using the following formula [17]:

$$d \geq \frac{2D^2}{\lambda} = \frac{2D^2 f}{c}$$

Here, D is the largest antenna dimension [m], f is the frequency of the signal [Hz] and c is the speed of light [$3 \times 10^8 m/s$]. For our case, these parameters are $D = 35mm$ from the datasheet [20], $23GHz \leq f \leq 33GHz$. Therefore, the far field distance is calculated as $17cm \leq d \leq 24cm$. As the maximum far field distance of the given antenna was 24 cm, the base height was set at 25 cm, to make sure that it would be in the far field region.

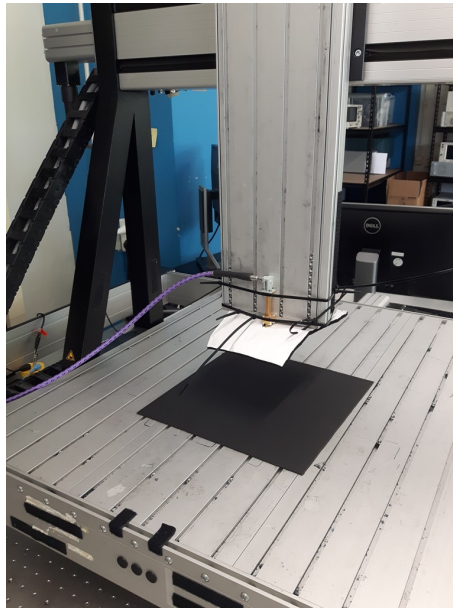


Figure 3.6: The used measurement setup

1. Calibrate the PNA with the attached cable, then connect it to the antenna
2. Fasten the antenna to the arm of CNC, so that it points vertically down.
3. Adjust the position of the arm to the centre of the absorber with a height of 25 cm.
4. Save the data shown on the screen.
5. Repeat step 3 to 4 for different heights. The heights used are from 10 cm to 35 cm with step size of 5 cm.
6. Processing all the data.

3.1.3. Codes Design

The codes of assessment should become a realization of the problem definition shown in Section 1.2.2. Therefore, the signals and the processing methods mentioned need to be converted into discrete signals and computer algorithms. The conversion can be found in Table 3.1

| Elements | Program Realization |
|----------------------------------------------|---------------------------------------|
| Frequency Domain Signals e.g. $X(f)$ | Discrete Frequency Waveform $X[n]$ |
| Discrete Time Domain Signals e.g. $g(nT)$ | Discrete Time Waveform $g[n]$ |
| DTFT | Fast Fourier Transform (FFT) |
| iDTFT | Inverse Fast Fourier Transform (IFFT) |
| Windowing Function $W(f)$ | Hamming window |

Table 3.1: Conversion

After this conversion, the MatLab codes with algorithm flow shown in 3.7 is designed. The main body is designed as the controlling part that passes right data set to "Analysis" function one by one. "Analysis" is a function that performs the data analysis described by Figure 1.3. The details are visible in Appendix A.

The algorithm above is implemented into both ADS and MATLAB. ADS simulation has advantage in preparing a set of simulation data and expected result. By comparing the results of ADS simulation and MATLAB result, we can ensure the MATLAB works as expected.

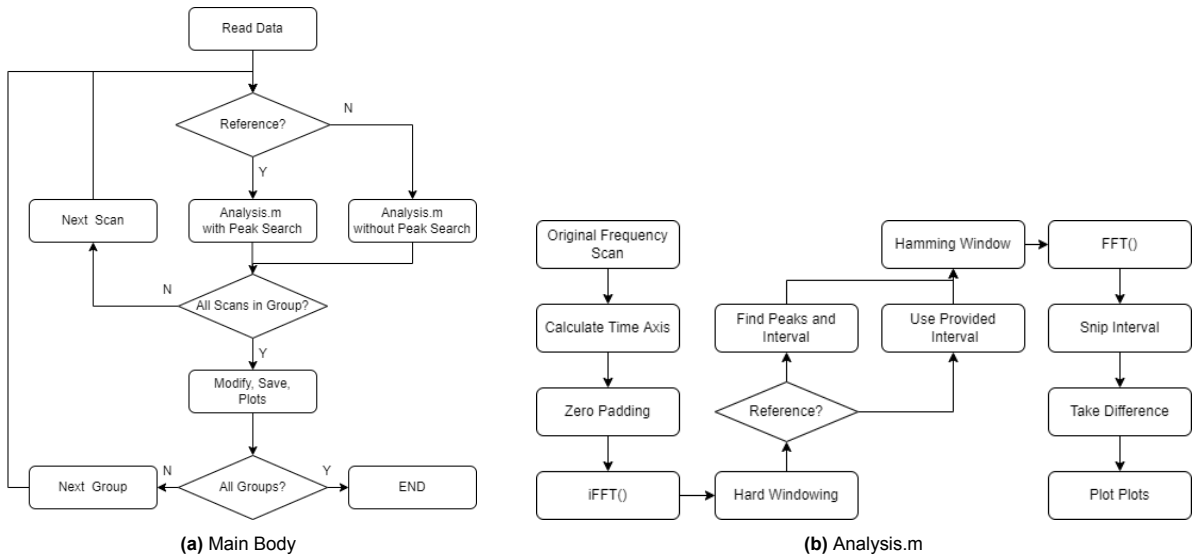


Figure 3.7: Algorithm Flow Chart

3.2. Faraday cage

The Faraday cage is realized by using $35\mu m$ thick copper tape [21], this since the skin depth of copper is smaller than that of aluminium, as depicted in section 1.3. Thus allowing more times the skin depth in the same thickness of tape.

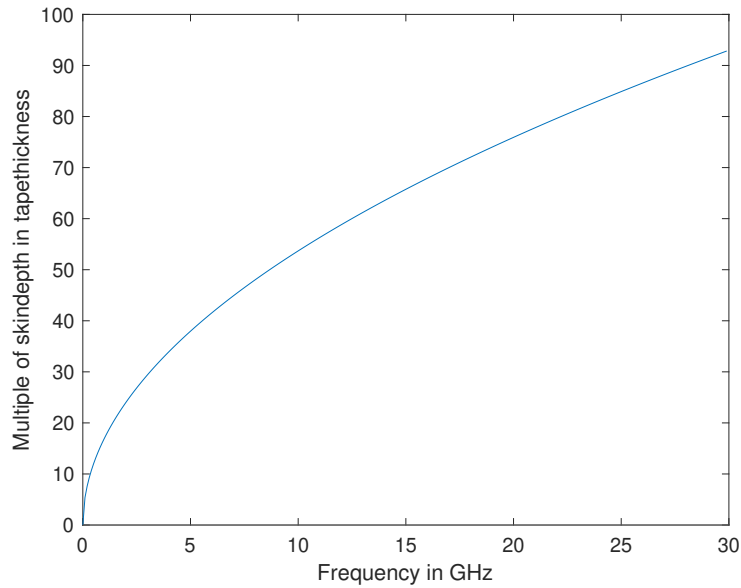


Figure 3.8: How much times the skin depth at the given frequency fits in the copper tape

In figure 3.8 it can be seen that from as low as 100 MHz there are already 5 times the skin depth in the thickness of the tape. However, this doesn't yield the same attenuation as mathematically predicted in section 1.3. The reason for this is that the copper tape parts after covering the inside of the dome are not forming a perfect conductor. Because the width of the tape is 50mm, and the strips of copper are only connected by the conductive adhesive layer as the tape strips were overlaid on each other. Here a note must be placed that the tape wasn't placed per panel due to time constrains. However, the modular principle can still be kept if each panel is prepared separately.

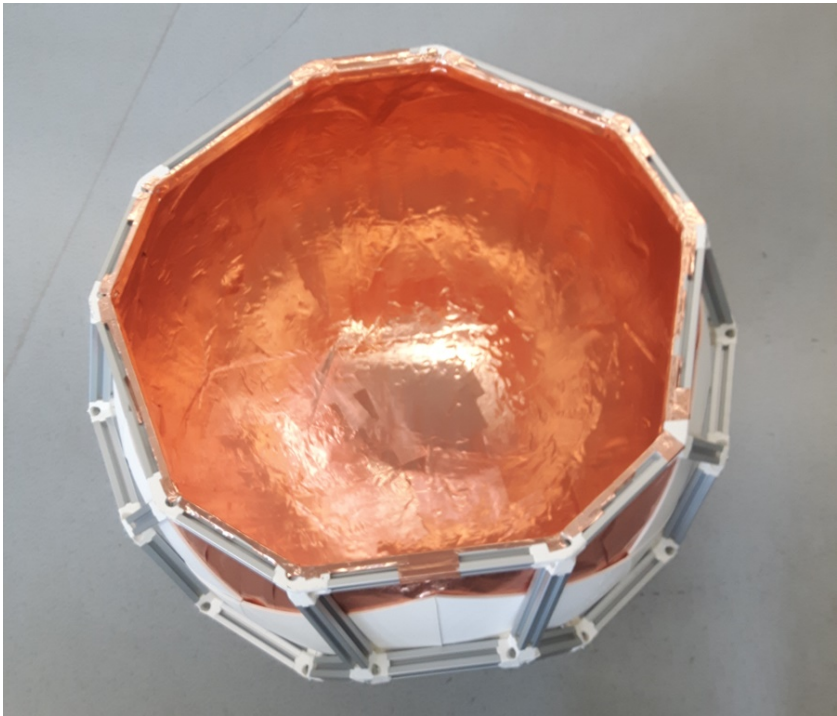


Figure 3.9: The inside of the minidome covered with the copper tape.

3.2.1. Physical Setup

Instruments

To test the shielding of the antenna dome chamber, following instruments were used: Geozondas probe antenna's 9-26 GHz, Rohde&Schwarz SMA100B Signal Generator and Agilent E4446A PSA Series Spectrum Analyzer.

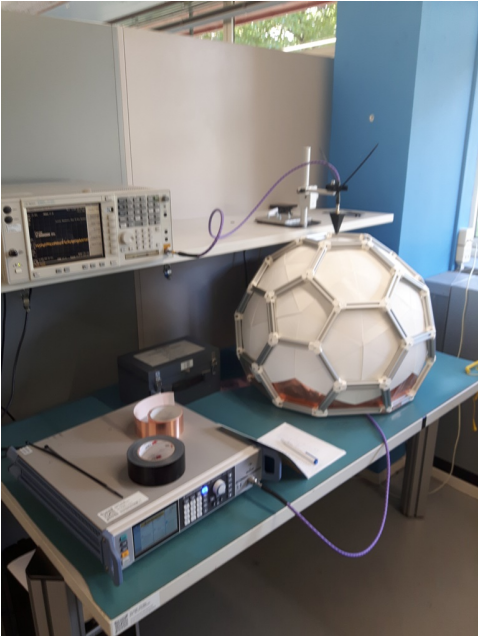


Figure 3.10: The used measurement setup

Measurement Procedure

The measurement procedure is described in the list below.

1. Connect one antenna to the signal generator. This antenna was placed inside the dome chamber.
2. Connect the other antenna to the spectrum analyser. This antenna was placed in a holder above the dome and oriented to the top of the dome.
3. The signal generator was set to an output power of 0 dBm, and manually swept from 15 to 38 GHz. And at every frequency step the received power by the spectrum analyser was recorded.
4. The measured power from the first series of data where there wasn't a Faraday cage were compared to the data after mounting a Faraday cage in the dome.

3.3. Anechoic Chamber

This section aims to explain the construction and assessment of the anechoic chamber. This section is further divided into 2 subsections. Subsection 3.3.1 shows the rebuilding process of the dome. Subsection 3.3.2 explains the assessment of the dome.

3.3.1. Rebuilding the Mini-dome

The chamber is based on an aluminium skeleton, with 3D printed connectors, as shown in Figure 3.11.

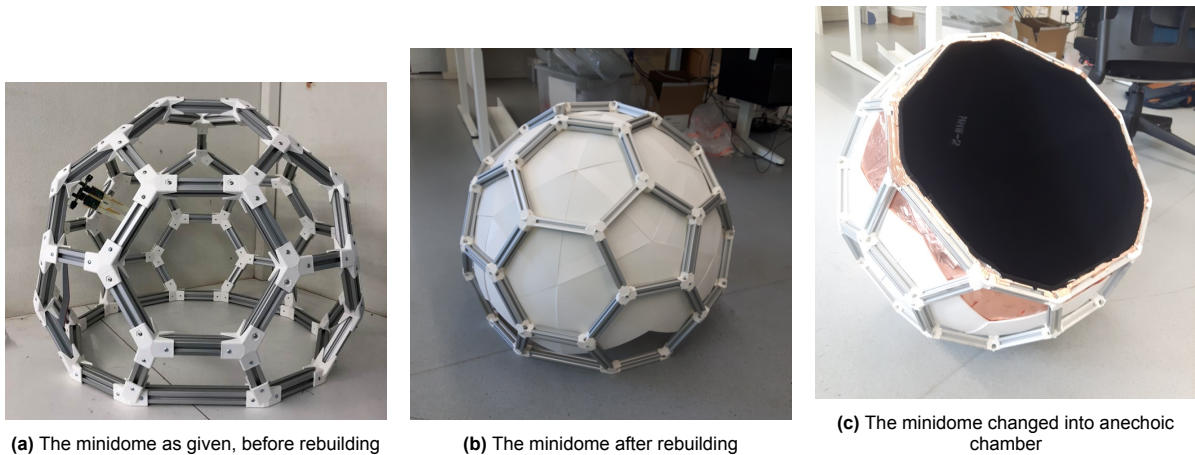


Figure 3.11: Different states of the minidome

Just as the latter design, the new dome is based as much as possible on a modular design for better convenience. However, new connectors were printed using FDM 3D print technique, these were needed since the old version wasn't able to hold the plastic interior panels (which were also printed using the same technique). As another improvement, the new design stiffened up the dome, as the connectors are bolted onto the cut face aluminium extruded profiles, which needed to be threaded on the inside. Whereas the old connectors were fastened inside the slot of the profile.

A cross-section of the dome can be seen in Figure 3.12. There is from the outside to the inside visible: the aluminium base structure to see in gray, then the plastic interior panels in white, the copper Faraday cage shielding in orange and last the absorber material in black.

This order was chosen especially, as the copper tape to shield the outside radiation was easy to apply to the panels, needed to be on the backside of the absorber and the modularity of the dome is now still accessible and panels are easier to replace (when the copper tape and absorber are applied per panel). Furthermore, the absorber needed to be placed closest to the AUT, that way the internal reflections are absorbed first, before getting to any source of disruption. Like for example that the dome would have if there wasn't an absorber placed, and only the copper tape was placed to shield outside radiation, which on the inside would give lots of reflections. This can also be seen in the data which is presented in section 4.2.

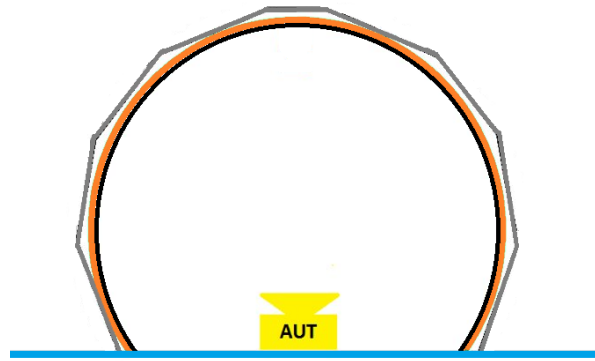


Figure 3.12: A cross-section of the dome

3.3.2. Assessment of the Anechoic Chamber

Instruments

To test the absorption of the antenna dome chamber, the following instruments were used: Geozondas probe antenna 9-26 GHz, Agilent N5242A 10MHz – 26.5GHz PNA-X Vector Network Analyzer.

Measurement Procedure

The measurement procedure is described in the list below.

1. Calibrate the PNA-X with the attached cable, then connect it to the antenna.
2. This antenna was placed inside the dome chamber.
3. Save the data shown on the screen.
4. The measured signal from the first measurement where the interior of the dome was the copper tape was compared to the data after covering the copper tape inside with the MMW-2 absorber in the dome.

4

Results

This chapter contains the results obtained from the experiments and data processing. This chapter contains two sections. Section 4.1 contains the results related to the assessment of the absorbing materials. Section 4.2 contains the results related to the assessment of the anechoic chamber.

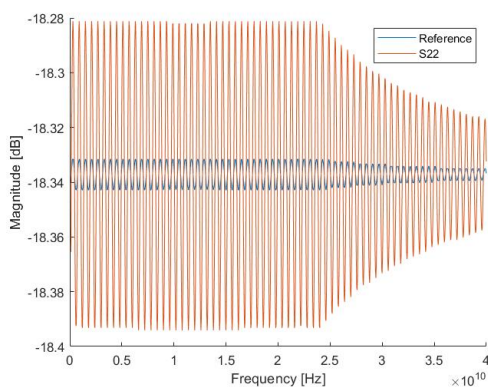
4.1. Absorbing Material Assessment

We followed the procedure described in Section 3.1.2 and successfully obtained several data. The data can be analysed from several directions: first we examined the influence of the distance to the reflection pattern, then the general absorbing effect with respect to the metal plate reference is summarized from the obtained data.

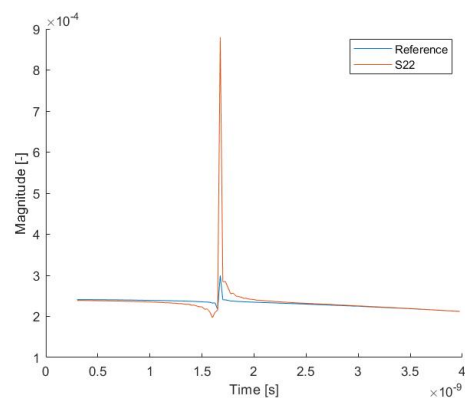
4.1.1. Verification of MatLab Codes

With simulation software ADS, an ideal data set is obtained. The ideal data and the further processing is shown in 4.1.

From the figures, it can be observed that despite the difference in forms due to different number of sample points, both results indicates the attenuation are -20 dB. This verifies that the algorithm can obtain the expected results.



(a) Original Data



(b) Time Domain Peaks

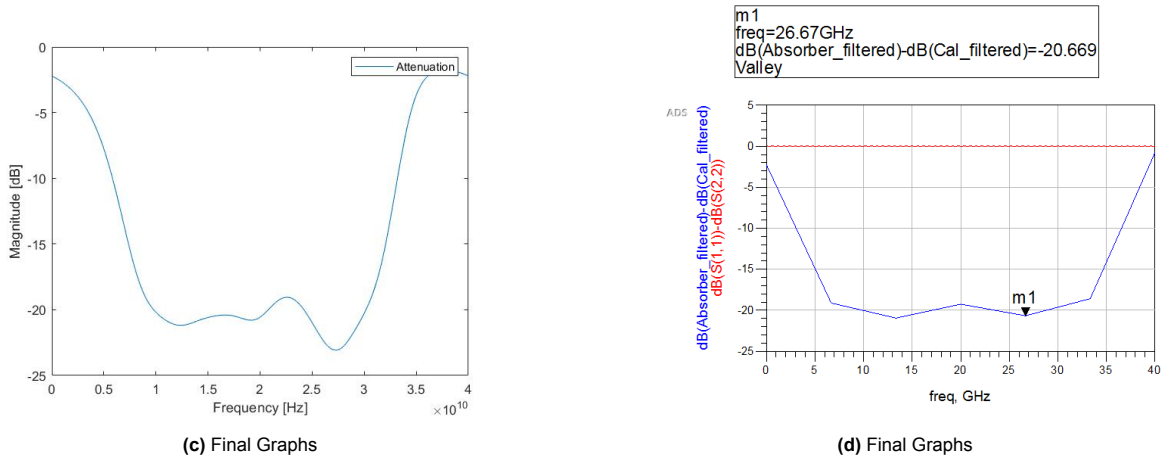


Figure 4.1: Processing of the Ideal Data

4.1.2. Time Gating

The aim of the time domain verification is to ensure that the right peak is processed by the algorithm. Two time domain plots are shown in Figure 4.2 as examples.

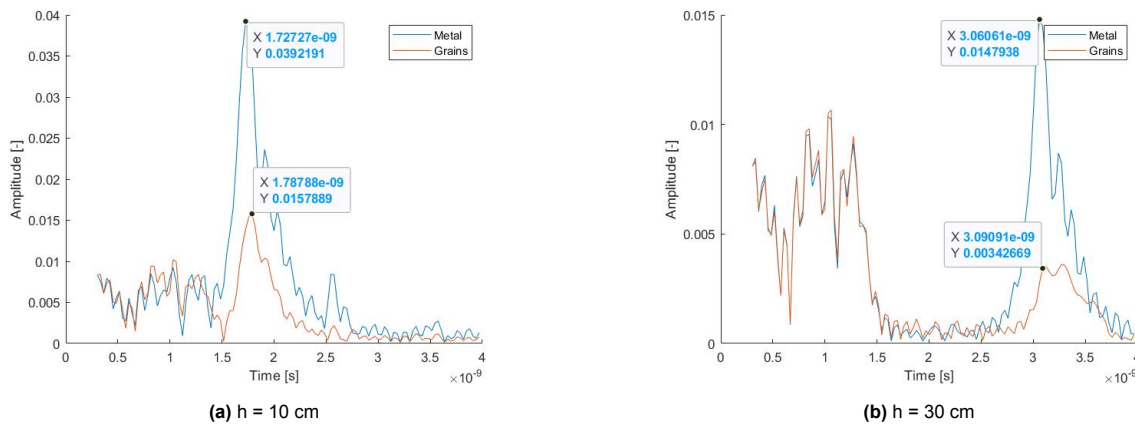


Figure 4.2: Two Examples of Peaks of Different Heights

Figure 4.2 is a segment of the whole time domain after iFFT. The snippet is chosen with an estimation of the ToA. Because the path lengths are $20\text{cm} \leq l \leq 70\text{cm}$, this segment is chosen as $10\text{cm} \leq l_e \leq 120\text{cm}$ in order to fully cover the signal peaks. The time range $0.33\text{ns} \leq t \leq 4\text{ns}$ is then calculated using Formula 1.3.

To the right of both graphs there are clear peaks from different signals. The center of all peaks are clear and well aligned, and the varied amplitudes of the signals imply the results of the transform from frequency domain to the time domain are seemingly correct.

In order to further verify the obtained signals, lengths of the travel paths need to be calculated. This is possible with a reference measurement, which is taken as the metal plate is placed right against the antenna. The ToA can be then approximately calculated by:

$$t_a = t_p - t_r$$

Here t_a is the ToA, t_p is the time value of the peak to be verified and t_r is the time value of the peak of the 0 cm reference. Then using formula $l = ct_a$, the approximate length of the travel path can be calculated, as shown in Table 4.1.

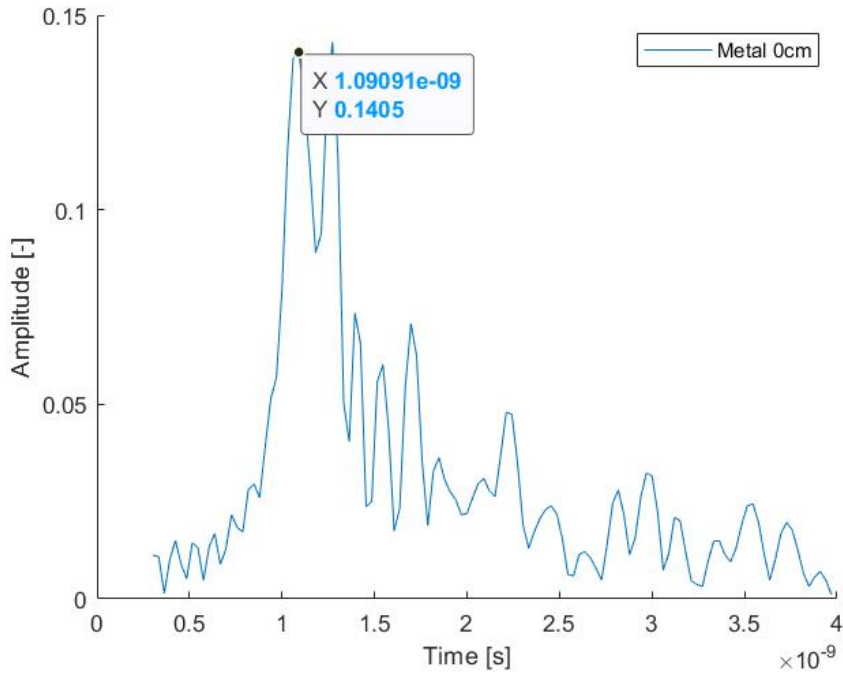


Figure 4.3: Reference at 0 cm

| h[cm] | t_p [ns] | ToA[ns] | l[cm] | 2*h[cm] | Error [cm] |
|-------|------------|---------|-------|---------|------------|
| 0 | 1.09 | 0 | 0 | 0 | 0 |
| 10 | 1.72 | 0.63 | 18.9 | 20 | 1.1 |
| 15 | 2.06 | 0.97 | 29.1 | 30 | 0.9 |
| 20 | 2.4 | 1.31 | 39.3 | 40 | 0.7 |
| 25 | 2.73 | 1.64 | 49.2 | 50 | 0.8 |
| 30 | 3.06 | 1.97 | 59.1 | 60 | 0.9 |
| 35 | 3.39 | 2.30 | 69.0 | 70 | 1 |

Table 4.1: Calculated Path Length

The calculated l has error with respect to the ideal path length. This can be explained by systematical error. Due to the impurity of the 0 cm reference as shown in Figure 4.2, all the graphs has a "hedgehog" like around time interval $t \in [0.5, 1.5]$ ns. This is probably caused by the inner reflection of the antenna. Despite the error in path length calculation, the ToA of the peaks under all distance is reasonable, which means the data passed the check of this part.

4.1.3. Absorbing Material Comparison

Following the steps described in Section 3.1.2, data shown in B.2 are obtained. Here the data with 25 cm height is taken as an example. The meaning of the labels in Figure 4.4 can be looked up in Table 4.2.

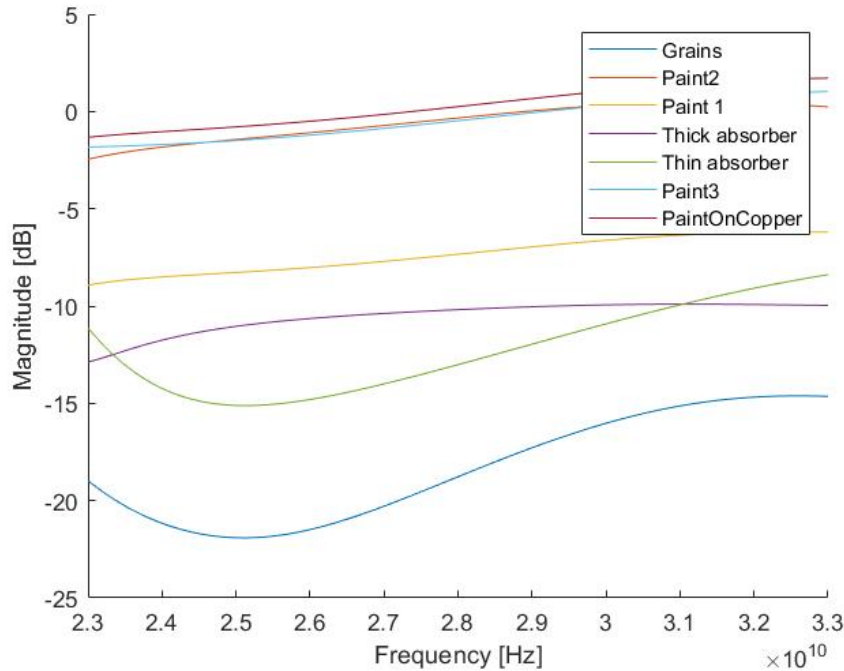


Figure 4.4: Analyse Result of data with $h = 25\text{cm}$ (a copy of B.2d)

| Labels | Explanation |
|-----------------|--------------------------------------------------------------------------------|
| Grains | Newly made absorbing metal plate with brushed paint and carbon grains of 2-5mm |
| Paint 2 | Newly made absorbing metal plate with brushed paint |
| Paint 1 | Existing sample with paints and carbon grains |
| Thick absorber | Absorbing pad MMW-2 |
| Thin absorber | Absorbing pad MMW-1 |
| Paint 3 | Newly made absorbing metal plate with rolled paint and carbon grains |
| Paint on Copper | Newly made absorbing plastic plate with copper tape, painted with roller |

Table 4.2: Look up Table of Figure B.2d

Figure 4.4 shows two clear classes of absorbing materials. Signals with labels 'Paint2', 'Paint3' and 'PaintOnCopper' show little absorbing attenuation. Remarks about this are placed in the discussion, which can be found in section 5.2. On the contrary, signals with labels "Thick absorber", "Thin absorber", "Paint 1" and "Grains" show different attenuation. Among them, the attenuation of "Grains" is the largest, which is as low as -20 dB.

However, Figure 4.4 shows unexpected pattern at high frequency. As shown in the graph, some traces show attenuation higher than 0 dB, which implies impossible phenomenon that the absorbing material amplifies the signal. One possible explanation is the windowing function brings unwanted rise to the trace at higher frequency. This problem is a part of the inaccuracy in the analysis.

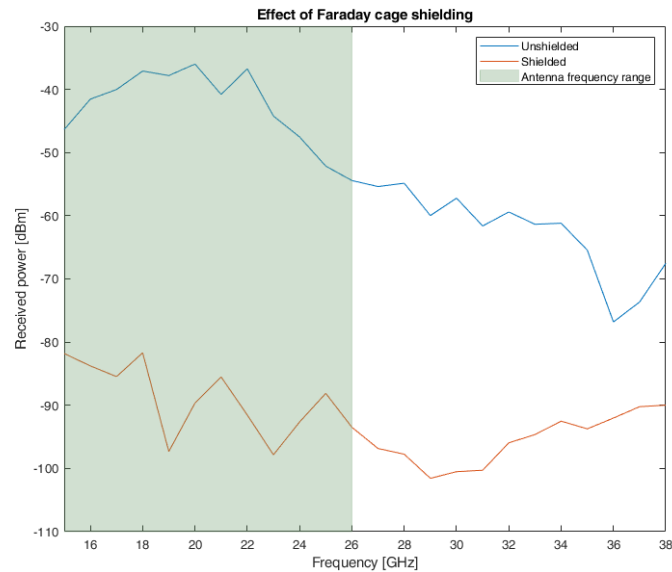
After examining other graphs with different distances, it is concluded that the relation of the absorbing properties varies, but the attenuation of "Thick absorber", "Thin absorber" and "Grains" are lower than other materials at all distances. The complete data can be found in Appendix B.2.

4.2. Assessment of the Chamber

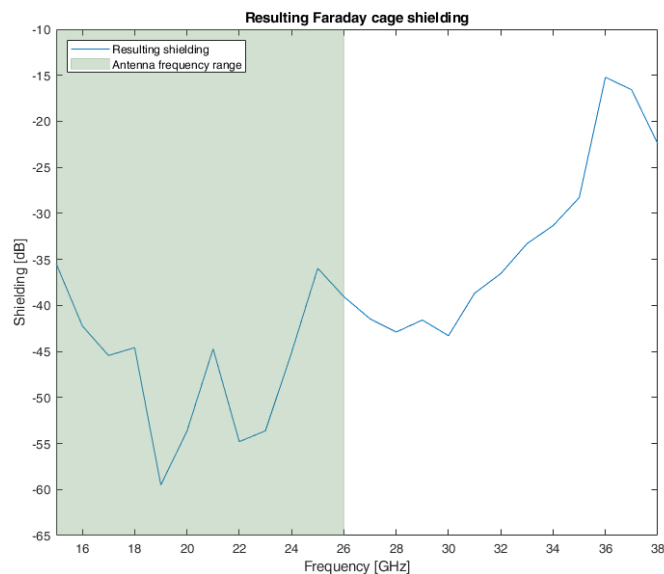
The assessment of the chamber consists of 2 subsections. First a section where the shielding from outside EM radiation is assessed, followed by a section where the attenuation from the absorber inside the dome is assessed.

4.2.1. Faraday shielding Measurement

The Faraday shielding test as discussed in section 3.2 reveals the attenuation created by the shielding effect. As shown in Figure 4.5b, the resulting shielding of the Faraday Cage is in the range of -15,2 dB to -59,5 dB. But a remark must be placed here, since the used antenna has a frequency range of 9 to 26 GHz, and in that range it can be said that the resulting shielding is at least -35 dB.



(a) Received power without and with the Faraday cage



(b) Shielding resulting from the Faraday cage

Figure 4.5: Faraday cage measurement results

4.2.2. S11 Measurement

The S11 Measurement, as discussed in section 3.3.2, shows the attenuation due to the absorbing material in the dome. The data processing yields Figure 4.6. As shown in Figure 4.6c, the general attenuation lies between -11.2dB and -10.9dB.

This result is comparable to the measurement data shown in Figure 4.4. Figure 4.4 indicates that the attenuation of this material which is referred to as 'thick absorber' in the figure. Hence, this material reaches the expected performance after it is put on the chamber.

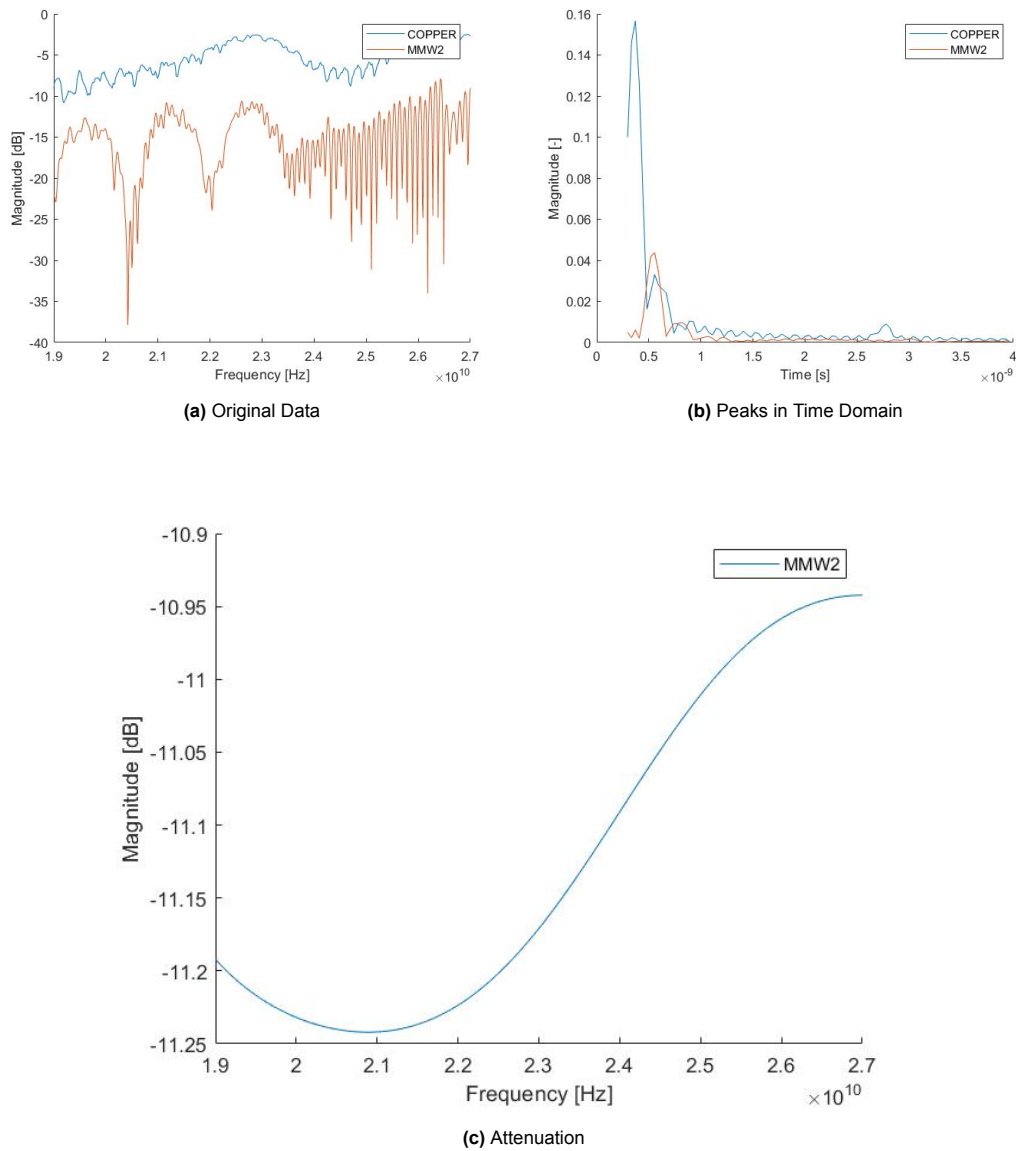


Figure 4.6: S11 Measurements of the Chamber

5

Conclusion and Discussion

5.1. Conclusion

After experiments on the absorbing materials, the absorbing properties of different materials are obtained. The measurement results of the absorbing materials suggest that the absorbing paint with the grains, which can reach as strong as -20 dB attenuation, has better absorbing effect than the absorbing pads. This result fulfil the requirements of the attenuation level, however it does not fulfil the requirement of the material assessment, as will be discussed in the next section.

Besides, the chamber with MMW2 absorbing material combined with the copper Faraday cage has decent absorbing and shielding effects. The shielding attenuation is stronger than -35 dB in the frequency range between 16 GHz and 32 GHz. And the internal reflection is attenuated by -11 dB, which as concluded in section 4.2.2 agrees with the measured plate data. Therefore, it can be concluded that the requirements in Chapter 2 are met.

5.2. Discussion

Because of the time constraints and the limitation of production capabilities, the best material chosen from material assessment is not always a good choice to be prepared on the chamber wands. For example, even though the paint with grains has the best performance at 25 cm, it is not chosen for the chamber because of its weight, sharp edges and the difficulties to get an even layer. Besides, preparing the interior panels will take large amount of time and large space, which makes it less applicable in the lab. Therefore, eventually MMW-2 material with a little weaker absorbing effect, but much less weight was put on the chamber. As from the slightly better absorbing MMW-1 material was too little available.

Besides, the tools for the preparation of the absorbing material also influence the experiment results. For example, the paint prepared by a roller is much thicker and more uniform than the one prepared by brushes. However, although at higher frequency of 28 GHz instead of 18GHz, as described in the data sheet [19], the result of around -2 dB attenuation are far from the given specifications of a -38 dB attenuation with one coat, and a -44 dB attenuation after 2 coats. A possibility could be that a thicker carbon layer is needed to absorb the radiation, since the layer thickness much smaller than the wavelength. Furthermore, there isn't any information given about the measurement setup that was used to get the attenuation rates in the datasheet, as the effect of the surface where the paint is applied could also have an effect on the result. But hence the little attenuation, eventually the paint only is not considered as an option.

Furthermore, the codes designed for analysis has large space of improvement in the data efficiency and clearance of structure. After reconstruction or development, it can also become a multi-functional analysis tool for more cases.

5.3. Recommendations

Regarding (the construction of) the dome/chamber, a few recommendations can be placed.

1. Foremost, it would be recommended to make a Bill of Materials, where all the required parts for assembly of the dome and anechoic chamber are placed onto. Also, here can the required specifications of each part be placed, insuring that the correct part(s) can be arranged for the required assembly step.
2. The new connectors that are mounted between the aluminium profiles are a structural improvement, however fitment is still important. This could for example be achieved to use a SLA 3D print technique, instead of the used FDM technique, as this has lower print tolerances. A comparison of this can be seen in figure 5.1.



(a) FDM print technique



(b) SLA print technique

Figure 5.1: A connector printed via different print techniques

3. Regarding the internal panels, a couple of remarks can be placed.

- (a) The interior panels have, due to the FDM print technique also play, as visible in figure 5.2. It could, especially with bigger diameter domes, be beneficial to fasten them together at the edges, to remove this play.

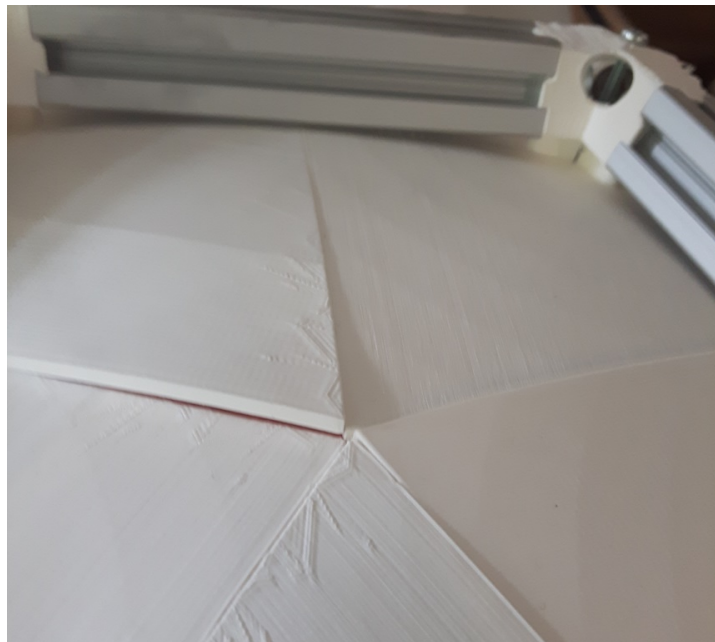


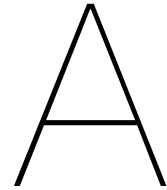
Figure 5.2: Visible height difference between the panels)

- (b) In the current STL file of the internal panel, 2 submeshes are used. This requires additional settings to make sure the connection between these submeshes are printed correctly. Especially setting up to print multiple panels at the same time, note should be taken.
 - (c) In the panels, there is a pocket on the inside of the panel for the nut. However, the nut is eager to misalign or fall out of it when mounting the panel. Furthermore, after using glueing copper tape or the absorber onto the panel, the nut is not accessible any more. To insure correct alignment and prevent the nut from falling, the nut could be glued into position, or a smaller pocket from the side can be used.
4. The lower ring of the dome has no panels fitted, to give additional support to the used copper tape and the absorber, it would be advised to design also panels that fit at those places. Since the gaps will need covered anyway to achieve the anechoic chamber. This will also ease the modularity.
 5. To reduce waste and given the time constrained, the internal panels were covered when mounted in the dome. This meant that larger pieces of copper tape and absorber could be used. Therefore, it is advised to test if using smaller pieces of the same size as the internal panels will not negative impact the achieved results.
 6. If the above stated smaller pieces of absorbers are used, an advice would be to make a template per panel, to ease cutting the copper tape and absorber to size.
 7. Finally, the chamber hasn't been tested with any sensing nodes inside. Further research on this is also recommended.

Bibliography

- [1] GrandViewResearch. "5g infrastructure market size, share & trends analysis report by component (hardware, services), by spectrum (sub-6 ghz, mmwave), by network architecture, by vertical, by region and segment forecasts, 2022 - 2030." (2022), [Online]. Available: <https://www.grandviewresearch.com/industry-analysis/5g-infrastructure-market> (visited on 06/12/2022).
- [2] K. A. Remley, J. A. Gordon, D. Novotny, *et al.*, "Measurement challenges for 5g and beyond: An update from the national institute of standards and technology," *IEEE Microwave Magazine*, vol. 18, no. 5, pp. 41–56, 2017. DOI: 10.1109/MMM.2017.2690882.
- [3] E. R. Hunter and T. Stander, "A compact, low-cost millimetre-wave anechoic chamber," pp. 1–5, 2016. DOI: 10.1109/EuCAP.2016.7482012.
- [4] Rohde&Schwarz. "Antenna beam characterization of 5g mobile devices and base stations using the r&s@nrpm over-the-air (ota) power measurement solution." (2022), [Online]. Available: https://www.rohde-schwarz.com/nl/applications/antenna-beam-characterization-of-5g-mobile-devices-and-base-stations-using-the-r-s-nrpm-over-the-air-ota-power-measurement-solution-application-note_56280-471745.html (visited on 06/12/2022).
- [5] F. Musters, "Real-time 3d characterization of antenna systems," M.S. thesis, Technical University of Delft, Aug. 2019.
- [6] W. Emerson, "Electromagnetic wave absorbers and anechoic chambers through the years," *IEEE Transactions on Antennas and Propagation*, vol. 21, no. 4, pp. 484–490, 1973. DOI: 10.1109/TAP.1973.1140517.
- [7] P. Niemand and J. Odendaal, "Characterization of radar-absorbing material using time-domain techniques," in *Proceedings of the 1998 South African Symposium on Communications and Signal Processing-COMSIG '98 (Cat. No. 98EX214)*, 1998, pp. 367–372. DOI: 10.1109/COMSIG.1998.736984.
- [8] N. Vohra and M. El-Shenawee, "K- and w-band free-space characterizations of highly conductive radar absorbing materials," *IEEE Transactions on Instrumentation and Measurement*, vol. 70, pp. 1–10, 2021. DOI: 10.1109/TIM.2020.3041821.
- [9] A. Ramírez-Arroyo, A. Alex-Amor, C. García-García, Á. Palomares-Caballero, P. Padilla, and J. Valenzuela-Valdés, "Time-gating technique for recreating complex scenarios in 5g systems," *IEEE Access*, vol. 8, pp. 183 583–183 595, Oct. 2020. DOI: 10.1109/ACCESS.2020.3028750.
- [10] M. Winebrand and J. Aubin, "Improving the accuracy of near-field antenna measurements using time-gating techniques," in *2010 14th International Symposium on Antenna Technology and Applied Electromagnetics & the American Electromagnetics Conference*, 2010, pp. 1–3. DOI: 10.1109/ANTEM.2010.5552388.
- [11] W. K. Jenkins, D. L. Jones, and B. J. Hunsinger, "28 - discrete-time signal processing," in *Reference Data for Engineers (Ninth Edition)*, W. M. Middleton and M. E. Van Valkenburg, Eds., Ninth Edition, Woburn: Newnes, 2002, pp. 28-1-28–39, ISBN: 978-0-7506-7291-7. DOI: <https://doi.org/10.1016/B978-075067291-7/50030-3>. [Online]. Available: <https://www.sciencedirect.com/science/article/pii/B9780750672917500303>.
- [12] P. Mathur and S. Raman, "Electromagnetic interference (emi): Measurement and reduction techniques.," *Journal of Electronic Materials*, vol. 8, Feb. 2020. DOI: 10.1007/s11664-020-07979-1.
- [13] I. TECHNOLOGY, *2017 emi shielding guide*, Brochure, 2017. [Online]. Available: https://interferencetechnology.com/wp-content/uploads/2017/06/2017_IT_EMI-Shielding-Guide_Low-Res.pdf.
- [14] J. L. et al., "Emi shielding technology in 5g rf system in package module," *IEEE 70th Electronic Components and Technology Conference (ECTC)*, pp. 931–937, 2020. DOI: 10.1109/ECTC32862.2020.00152.

- [15] X. Z. L. Yan L. Xu and R. X. Gao, "An angularly stable frequency selective surface with vent holes for 5g electromagnetic shielding," *International Symposium on Electromagnetic Compatibility - EMC EUROPE*, pp. 366–369, 2019. DOI: 10.1109/EMCEurope.2019.8872122.
- [16] R. W. Evans, *Design guidelines for shielding effectiveness, current carrying capability, and the enhancement of conductivity of composite mater*, NASA Contractor Report, 1997. [Online]. Available: <https://ntrs.nasa.gov/api/citations/19970036055/downloads/19970036055.pdf>.
- [17] D. M. Pozar, in *Microwave engineering*. Wiley, 2012.
- [18] CumingMicrowave. "Datasheet mmw absorbers." (2022), [Online]. Available: <https://www.cumingmicrowave.com/pdf/Application%5C%20Notes/AN300-13%5C%20C-RAM%5C%20MILLIMETER%5C%20WAVE.pdf> (visited on 06/12/2022).
- [19] GigahertzSolutions. "Datasheet cfa40-5 shielding paint." (2015), [Online]. Available: https://www.gigahertz-solutions.de/media/pdf/fe/f0/68/863-091_Manual_CFA40_INT.pdf (visited on 06/12/2022).
- [20] FlannMicrowave. "Standard gain horn series 240 (data sheet)." (2016), [Online]. Available: <https://flann.com/wp-content/uploads/2022/05/Series-240-Datasheet.pdf> (visited on 06/12/2022).
- [21] WurthElektronik. "Datasheet 3003350a conductive metallic tape." (2016), [Online]. Available: <https://www.we-online.com/katalog/datasheet/3003350A.pdf> (visited on 06/12/2022).



Source Code

A.1. Functions

A.1.1. AssembleComplex

```
1
2 function ArrayOut = AssembleComplex(ArrayIn,option)
3 %ASSEMBLECOMPLEX can convert two array of [magarray,phasearray] into
4 %[complexarray]. Which has different options to fit different data
5 %Input:
6 %   ArrayIn: n by 2 array to be assembled. Should be [Mag,Phase];
7 %           OR n by 1 array to be converted. Should be [Mag]
8 %   option: Type of data. Choose among: {"MagAngle","RealComplex","dBAngle"}
9 %           When ArrayIn is 1d, choose among:{"Mag","dB"}
10 if (length(ArrayIn(1,:))==2)
11     if option=="MagAngle"
12         ArrayOut=ArrayIn(:,1).*exp(1j.*ArrayIn(:,2).*pi/180);
13     else
14         if option=="RealComplex"
15             ArrayOut=ArrayIn(:,1)+1j.*ArrayIn(:,2);
16         else
17             if option=="dBAngle"
18                 ArrayOut=exp(ArrayIn(:,1)/10).*exp(1j.*ArrayIn(:,2).*pi/180);
19             else
20                 disp("Error2: Option not found for 2d array");
21                 ArrayOut=[NaN];
22             end
23         end
24     end
25 end
26
27
28 else
29     if (length(ArrayIn(1,:))==1)
30         if (option=="dB")
31             ArrayOut=exp(ArrayIn(:,1)/20);
32         else
33             if (option=="Mag")
34                 ArrayOut=ArrayIn;
35             else
36                 disp("Error3: Option not found for 1d array");
37                 ArrayOut=[NaN];
38             end
39         end
40     else
41         disp("Error1:Dimension mismatch. Use 1d or 2d(n,2) Array")
42     end
43 end
44
45 end
```

A.1.2. Analysis

```

1
2
3 function [RefOut,ReturnInterval,ResultIFFT]=Analysis(FreqAxis,RefIn,Test,SearchInterval,Delay
   )
4 % Analysis carries out analysis. Results are in plot 1 to 6
5 % In:
6 %   FreqAxis: 1 by n array of frequency axis
7 %   RefIn: Reference Signal in time domain. Use [] if input should be reference
8 %   Test: Signal to be processed
9 %   SearchInterval: Search interval of peaks. Use [] if input should be reference
10 %   Delay: To delay the plot. Can be ignored
11 %Out:
12 %   RefOut: Generated Reference Signal snippet.
13 %   ReturnInterval: Generated Search Interval
14 %   ResultIFFT: Result signal of FFT
15
16 %Calculate time axis and zero padding
17 Fstart=FreqAxis(1);
18 Fend=FreqAxis(length(FreqAxis));
19 width=10;
20 zerosadded=floor(Fstart/((Fend-Fstart)/(length(FreqAxis)-1)));
21 TimeStep=1/(Fend); %sample frequency of frequency plot
22
23 %Zero padding and IFFT
24 paddedTest=[zeros(zerosadded,1);Test];
25 TD=ifft(paddedTest);
26 %Check if delay is needed
27 if exist("Delay","var")
28     TD=[TD(Delay:length(TD));zeros(Delay-1,1)];
29 end
30
31 %Estimated interval. To avoid start and end of IFFT. Points in the
32 %interval is kept and the rest are removed
33 distmax=1.2;
34 distmin=0.1;
35 TravelInterval=floor(distmin/(3*10^8)/TimeStep):floor(distmax/(3*10^8)/TimeStep);
36 Mask=zeros(size(TD));
37 Mask(TravelInterval)=1;
38 TDCut=TD.*Mask;
39
40 %Find the peak in either given interval, or previous interval. If latter,
41 %give interval around the peak in ReturnInterval
42 if isempty(SearchInterval)
43     [~,peakInd]=max(abs(TDCut));
44     ReturnInterval=max((peakInd-width),1):(peakInd+width);
45 else
46     ReturnInterval=SearchInterval;
47     peakInd=SearchInterval((length(SearchInterval)-1)/2);
48 end
49 %Windowing with hamming window
50 W=hamming(width);
51 windowinterval=(peakInd-width/2+1):(peakInd+width/2)';
52 Mask2=zeros(size(TD));
53 Mask2(windowinterval)=W;
54 PeakCut=TD.*Mask2;
55 %FFT
56 Filtered=fft(PeakCut);
57
58 %Put filtered out if input should become a reference
59 if isempty(RefIn)
60     RefOut=Filtered;
61     PrintPlot=0;
62 else
63     RefOut=RefIn;
64     PrintPlot=1;
65 end
66
67 %Plot Everything. Time domain is abs-t and frequency domain is dB-f.
68 %Can also put c*t in the x axis

```

```

69 figure(1);
70 hold on;
71
72 plot(FreqAxis,mag2db(abs(Test)));
73
74 figure(2);
75 hold on;
76
77 TimeAxis=(0:TimeStep:(length(TD)-1)*TimeStep)';
78 spaceAxis=TimeAxis.*3*10^8;
79 plot(TimeAxis,abs(TD));
80 figure(3);
81 hold on;
82 plot(TimeAxis(TravelInterval),abs(TDCut(TravelInterval)));
83
84 figure(4);
85 hold on;
86 plot(TimeAxis(windowinterval),abs(PeakCut(windowinterval)));
87
88 figure(5);
89 hold on;
90 NewFreqAxis=0:(Fend-0)/(length(PeakCut)-1):Fend;
91 plot(NewFreqAxis,mag2db(abs(Filtered)));
92 %Don't plot if it need to be a reference.
93 figure(6);
94 hold on;
95 Comp=mag2db(abs(Filtered))-mag2db(abs(RefOut));
96 minIndex=find(NewFreqAxis==Fstart);
97 maxIndex=length(NewFreqAxis);
98 ResultIFFT=[NewFreqAxis(minIndex:maxIndex)',mag2db(abs(Filtered(minIndex:maxIndex)))];
99 if (PrintPlot==1)
100 plot(NewFreqAxis(minIndex:maxIndex),Comp(minIndex:maxIndex));
101 end
102 %plot(abs(Ffiltered));
103 end

```

A.2. Scripts

A.2.1. DataAssemble

```

1
2 %Run this one to order all collected data plots
3 %Strings1 is material name
4
5 Strings1=["Metal_","Grains_","Paint2_","Reference - metal sheet_","Paint 1_","Thick absorber_","Thin absorber_","Metal2_","Paint3_","PaintOnCopper_"];
6 Strings4=".csv";
7 %Store all data
8 AllData=zeros([1001,1]);
9 LookUp=[];
10 DistStr=[];
11 addpath("3Jun2022","9Jun2022");
12 %Loops to scan different plots
13 for ind1=1:length(Strings1)
14     for ind2= 10:5:35
15         %make a file name base on material and distance
16         filename=Strings1(ind1)+string(ind2)+"cm";
17
18         if exist(filename+Strings4,"file")
19             Imported=importdata(filename+Strings4);
20             LookUp=[LookUp,filename];%it contains description to data of the same
                position
21
22
23             if (ind1==1)&&(ind2==10)
24                 AllData=Imported.data(:,1);
25             end
26             ComplexIn=AssembleComplex(Imported.data(:,2:3),"dBAngle");
27             AllData=[AllData,ComplexIn];
28         end

```

```

29
30
31     end

```

A.2.2. RunAnalysis

```

1 LegendStrings=[];
2 LegendStrings6=[];
3 TitleString=["Original Data ", "Ifft" , "TDCut", "PeakCut", "fft", "Compared to Ref"];
4 GraphType=["dB-f", "abs-t", "abs-t", "abs-t", "dB-f", "dB-f"];
5 DistStr=string(10:5:35)+"cm";
6 close all;
7 First=1;
8 Groups={1:3,4:7,8:10};
9 %Groups={1:10};
10
11 for ind1=2:7
12     for indG=1:length(Groups)
13         %Run Analysis in one group
14         for ind2=cell2mat(Groups(indG))
15             if (First==1) %This one is the reference
16                 First=0;
17                 [RefCut, Interval]=Analysis(AllData(:,1), [], AllData(:, ind1+(ind2-1)*6), []);
18                 Strings=erase(LookUp(ind1+(ind2-1)*6-1), "_" + DistStr(ind1-1));
19                 LegendStrings=[LegendStrings, Strings];
20
21             else %This one needs to be compared to reference
22                 Analysis(AllData(:,1), RefCut, AllData(:, ind1+(ind2-1)*6), Interval);
23                 Strings=erase(LookUp(ind1+(ind2-1)*6-1), "_" + DistStr(ind1-1));
24                 LegendStrings=[LegendStrings, Strings];
25                 LegendStrings6=[LegendStrings6, Strings];
26
27             end
28
29         end
30         First=1;
31
32     end
33
34 %Add plots elements
35     for ind2=1:length(TitleString)
36         figure(ind2);
37         if (ind2==6)
38             legend(LegendStrings6, 'Interpreter', 'none');
39         else
40             legend(LegendStrings, 'Interpreter', 'none');
41         end
42         %title(TitleString(ind2));
43         XYlabels=split(GraphType(ind2), "-");
44         switch XYlabels(1)
45             case "dB"
46                 ylabel("Magnitude [dB]");
47             case "abs"
48                 ylabel("Magnitude [-]");
49         end
50         switch XYlabels(2)
51             case "t"
52                 xlabel("Time [s]");
53             case "dist"
54                 xlabel("Travel Distance of Light [m]");
55             case "p"
56                 xlabel("Sample Points");
57             case "f"
58                 xlabel("Frequency [Hz]");
59         end
60
61         saveas(figure(ind2), "Group"+indG+"-"+DistStr(ind1-1)+"("+TitleString(ind2)+").fig");
62         clf('reset');
63     end

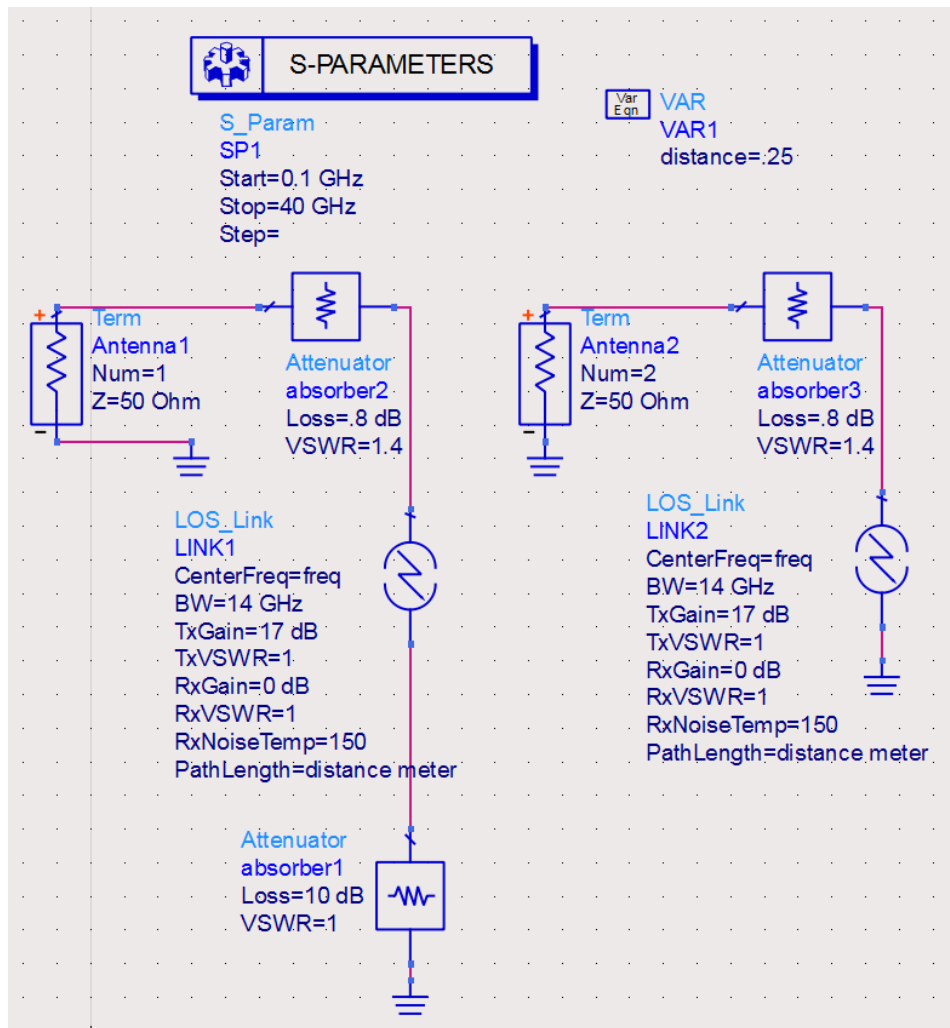
```

```
64
65 %empty legend strings
66 LegendStrings6=[];
67
68 LegendStrings=[];
69 end
70 close all;
```

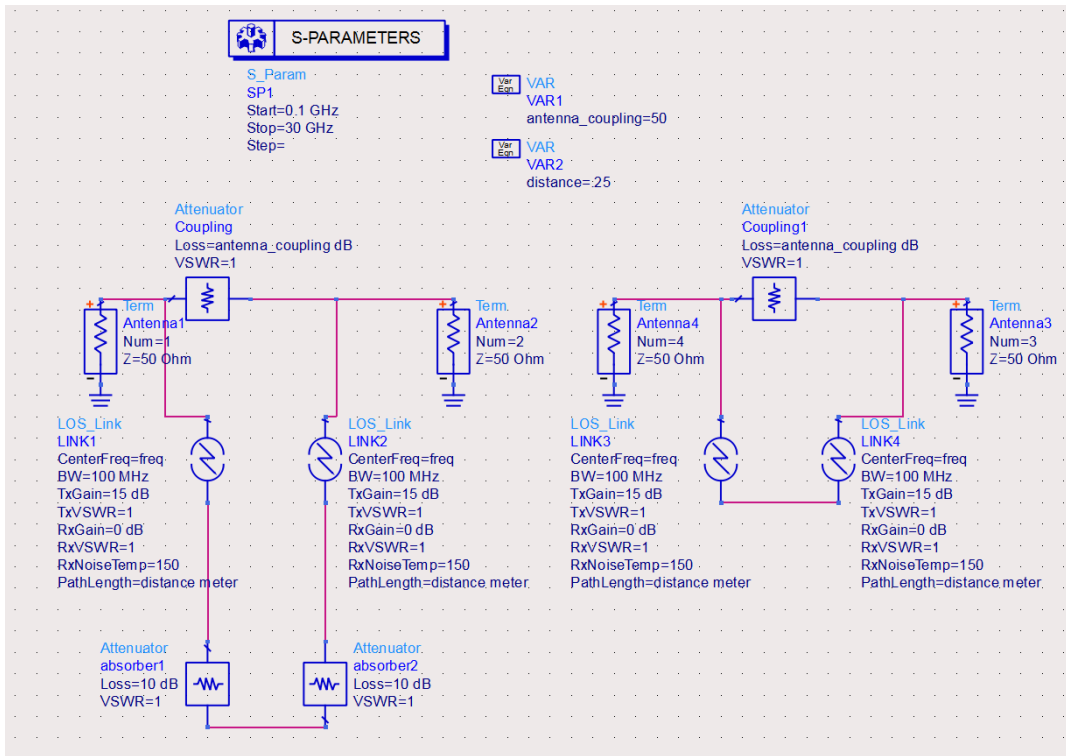
B

Additional Data

B.1. Addition Data of Simulations



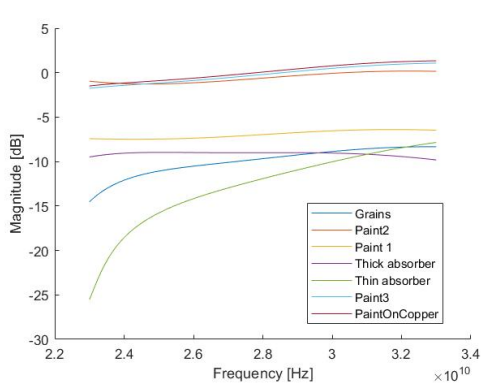
(a) Simulation of single antenna setup



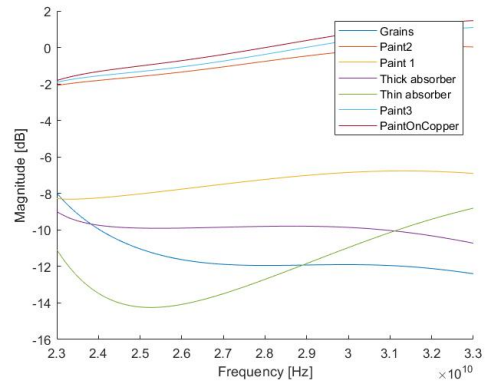
(b) Simulation of dual antenna setup

Figure B.1: Possible antenna setups to test the absorber

B.2. Addition Data of Absorbing Materials



(a) 10cm



(b) 15cm

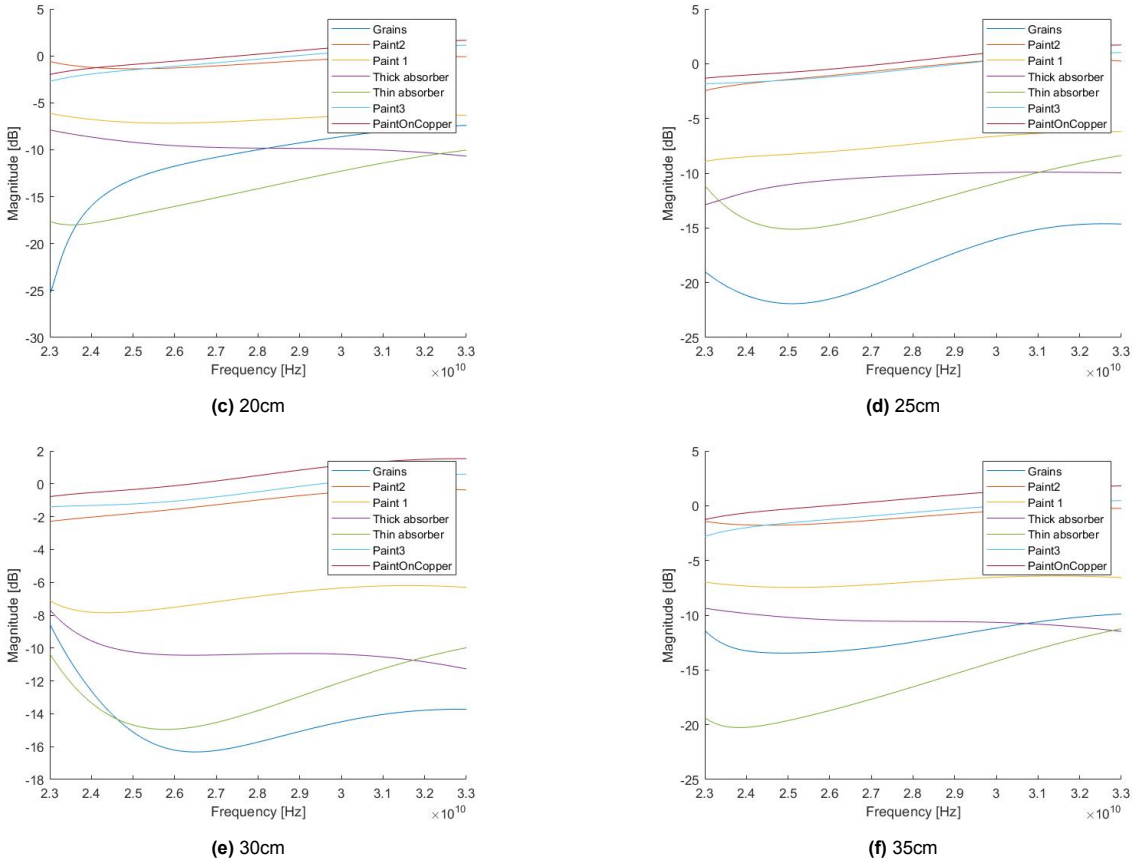


Figure B.2: Results of Different Distances